

High Speed and Precision Cutting of Thin Glass with Ultra-fast Asymmetric Bessel-like Beams

Lunzhen Hu^{1,2}, Quan Tang^{1,2}, Yetao Liu¹, Yuqiang Hou¹, Hao Zhang³, Evgeny L Gurevich^{1,4}, and Qingchuan Guo^{*1,2}

¹Center for Lasers and Optics, Green Industry Innovation Research Institute, Anhui University, Hefei 230088, PR China

²Information Materials and Intelligent Sensing Laboratory of Anhui Province, Anhui University, Hefei 230088, PR China

³School of civil aviation, northwest polytechnical university, Xian, 710072, PR China

⁴Laser Center (LFM), University of Applied Sciences Münster, Stegerwaldstraße 39, 48565 Steinfurt, Germany

*Corresponding author's e-mail: Qingchuan.guo@ahu.edu.cn

Ultra-white glass is widely used in industries such as display panels and automotive manufacturing. In order to meet the requirements of these industries for high-speed and high-quality glass cutting, asymmetric Bessel-like beams generated by cylindrical lenses are used to optimize the glass dicing process in this study. Single-shot intra-volume laser modifications in the low-iron glass with a thickness of 1 mm are performed followed by process parameter optimization. Through experimental research and theoretical analysis, the effects of defocusing distance, cutting speed (hole spacing), and laser power on the cutting quality of glasses are discussed. The results of symmetric and asymmetric Bessel beam cutting are compared, which demonstrates that the modified optic path offers significant advantages in terms of cutting speed and quality. By using an infrared picosecond laser with a wavelength of 1064 nm, combined with a CO₂ laser as a splinter tool, the minimum surface roughness of 0.6 μm was obtained when the cutting speed is 400 mm/s for the symmetric beam, and the higher cutting speed of 900 mm/s was achieved based on the asymmetrical beam with the minimum surface roughness of 0.6 μm . These results show that the asymmetric Bessel-like beam can significantly improve the cutting speed, which has an important application prospect in the straight-line cutting of glass.

DOI: 10.2961/jlmn.2025.01.2005

Keywords: ultra-fast laser, glass cutting, high speed, asymmetric, Bessel-like beams, roughness

1. Introduction

With its high transparency, no color distortion, and excellent optical performance, ultra-white glass has become the "star" material in the optical and construction industries and has been widely used in optical instruments, solar photovoltaic industry, display panels, and integrated electronics [1-5]. During the manufacturing process of such applications, the glass material needs to be cut according to the requirements. The key to obtaining good glass cutting quality is to reduce the fragmentation of edges and the roughness of glass cutting samples [6-9].

The conventional glass-cutting method mainly uses a diamond or carbide grinding wheel to cut the glass surface, and then apply mechanical breaking force, so that the glass along the scratches is completely separated. However, the mechanical cutting will leave considerable mechanical stress on the edge of the glass and the cutting edge is not necessarily perpendicular to the glass surface [10]. The subsequent breaking steps will cause small gaps and debris. In order to prevent the glass from breaking, it also needs to be grinding, polishing, and cleaning, resulting in an increase in the processing cost. Another glass-cutting method is high-pressure water-jet-cutting [11-12]. Compared with mechanical cutting, the heat generated in the cutting process can be taken away by water, so there is

no stress on the edge caused by thermal deformation. However, the price of high-pressure pumps and nozzles is expensive, and the accuracy and quality are limited by the diffusion and deflection of water. Moreover, glass is getting thinner, which in turn increases the difficulty of processing using conventional methods.

In recent years, laser precision processing has become a research hotspot in glass cutting due to its advantages of high precision, non-contact, and high energy density. The methods mainly include laser ablation, laser filamentation, and pulsed lasers based on Bessel beams [13]. However, the Rayleigh length of the Gaussian beam is relatively short. Therefore, the material removal rate in a single scan is very low and repeated scanning greatly reduces the processing efficiency [14-15]. Laser filamentation cutting is mainly applied with an ultra-short pulse laser to achieve a dynamic balance between the nonlinear self-focusing effect and the plasma-defocusing effect inside the glass medium [16-18]. Through the appropriate beam focus optical components, the light beam will not obviously diverge and will spread several times longer than the distance of the Rayleigh length. This method realizes the synchronous improvement of the cutting efficiency and quality of thin glass [19]. However, the thickness of the glass that can be processed is limited, so the cutting of thick glass cannot be realized [20].

Moreover, laser filamentation has high requirements for laser pulse intensity uniformity. In contrast, the Bessel beam has a long non-diffraction length, and its transverse light field distribution does not change with the propagation of the beam [21]. The main lobe diameter can be as small as a few micrometers, but the focal depth is up to several millimeters [22], which makes it easy to separate the glass at the laser-modified section by adding only a slight external force or thermal stress gradient [23]. Some research results prove that the Bessel beam has great advantages in glass cutting. The effects of different laser parameters on cracks and surface roughness are also studied [24-25]. In addition, the asymmetric Bessel beam extends these advantages even further [26]. Axicon lenses [27] are one of the most convenient and efficient tools for the Bessel beam generation. Asymmetric modifications in glass are widely investigated nowadays [28-31]. However, it is necessary to conduct a more detailed study about the effect of laser processing parameters on cutting quality.

Generally speaking, laser cutting speed is subject to laser power and repetition frequency. In our previous work [32], a picosecond laser with a high peak power and a long focal-depth Bessel beam was used to realize the linear cutting and special-shaped cutting of ultra-white glass with a cutting speed of 300 mm/s. Because the maximum speed limit of the machine is 1000 mm/s, the cutting speed has a lot of room for improvement. In this paper, asymmetric Bessel-like beams generated by cylindrical lenses are used to optimize the glass-cutting process. The effect of cutting speed, laser power, and defocusing distance on the surface roughness of the cross-sections are investigated. Defocusing distance is defined as the distance between the middle of the glass sample and the middle of the Bessel beam focal depth. When the central section is located below the middle of the glass, the value is positive. Otherwise, it is negative. The results of glass cutting with a thickness of 1 mm under symmetric and asymmetric Bessel beams are compared, showing that the asymmetric Bessel beam can significantly improve the cutting speed, and plays an important role in the process of high-speed cutting glass.

2. Experimental setups

2.1 Laser systems

The experiments were performed using picosecond laser systems emitting Gaussian laser pulses (10 ps, 1064 nm, $M^2 < 1.3$) and an axicon-based Bessel beam generation setup to produce strong material modification. The maximum output power is 50 W at a repetition rate of 200 kHz with a single pulse energy of 250 μ J. A laser source can be used in burst mode with 1-10 adjustable which allows the material to be irradiated with closely spaced pulse packets instead of a single pulse. The use of multiple burst modes avoids excessive ablation of high energy on the surface of the material, but as the number of pulses further increases, the single pulse energy of the sub-pulse is further weakened, resulting in insufficient ablation of the material and ineffective utilization of laser energy. Therefore, the number of sub-pulses is 4 (B4) with a repetition rate of 50 kHz was adopted in our experiment. The energy ratio of sub-pulses is 10:7:5:3 and the time interval of sub-pulses is 10:7:5:3 and the time interval of

the sub-pulse ($\Delta\tau$) is 33 ns. It also maintains the maximum output power of the ultrafast laser, and the total energy of the entire laser packet, which is determined by the laser power and repetition rate, is fixed at 1 mJ. The laser also has position synchronized output (PSO) function, which ensures that the laser is triggered at a constant space (rather than time) interval and that the pulse energy is uniformly applied to the processed object at all stages of the motion trajectory, including acceleration, deceleration, and uniformity.

The laser spot diameter is 2.5 mm and a 3X beam expander is used to expand the laser beam. After passing through the Bessel cutting lenses (from Evenoptics) with a maximum entrance beam of 8 mm, focal depth of 8 mm, and working distance of 15 mm, a symmetric round light spot with a diameter of 3 μ m was formed at the focus. As a result, the Bessel beam with high peak power density is generated inside the glass, instantly vaporizing the interaction area of material to produce a gasification zone, which rapidly diffuses to the upper and lower surfaces to form a hole. After cutting, a CO₂ laser beam (Synrad, ti100HS) with a maximum output power of 100 W is applied along the cutting line to form thermal stress and separate the glass. The schematic diagram of the picosecond laser with symmetric Bessel beam and asymmetric Bessel beam cutting glass experimental system is shown in Figure 1.

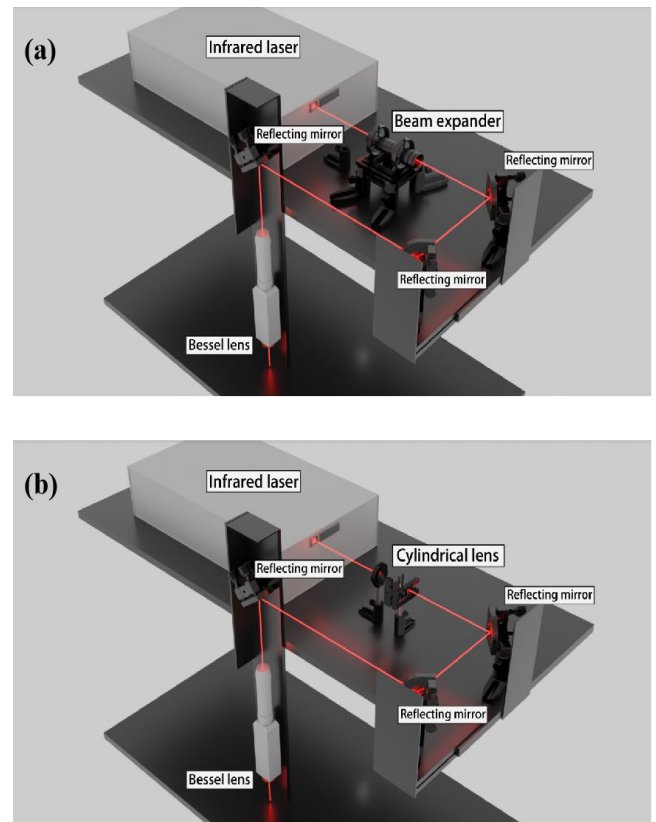


Fig. 1 Schematic diagram of picosecond laser with symmetric Bessel beam (a) and asymmetric Bessel beam (b) for laser glass cutting.

In addition, an elliptical Bessel beam is generated by two cylindrical mirrors with different focal lengths (parameters in Table 1) in front of the Bessel cutting lenses. The long axis of the ellipse is in the same direction as the cutting. The beam profile monitor (Changchun New Industries Optoelectronic Tech CN0307NIR-XN50-1064) which can measure diameters in the range of 1.0 to 100 μm was used to measure the light spot at the focal point, as shown in Figure 2 and Table 2. The diameter of a symmetric Bessel beam is about 1.6 μm . After passing two cylindrical mirrors, the morphology of the spot changes, and the elliptical Bessel spot is formed. The length of the asymmetric Bessel beam in the direction of the long and short axes is about 4.3 μm and 1.3 μm , respectively. After a large number of glass cutting experiments, the focal depth of the symmetric Bessel beam and asymmetric Bessel beam is judged to be 8 mm and 5 mm.

Table 1 Parameters about two cylindrical mirrors.

Parameter	Focus Distance	Center thickness	Radius	Flange Distance
Lens-1	50mm	2.77mm	25.85mm	48.19mm
Lens-2	-25mm	2.00mm	-12.93mm	-26.2mm

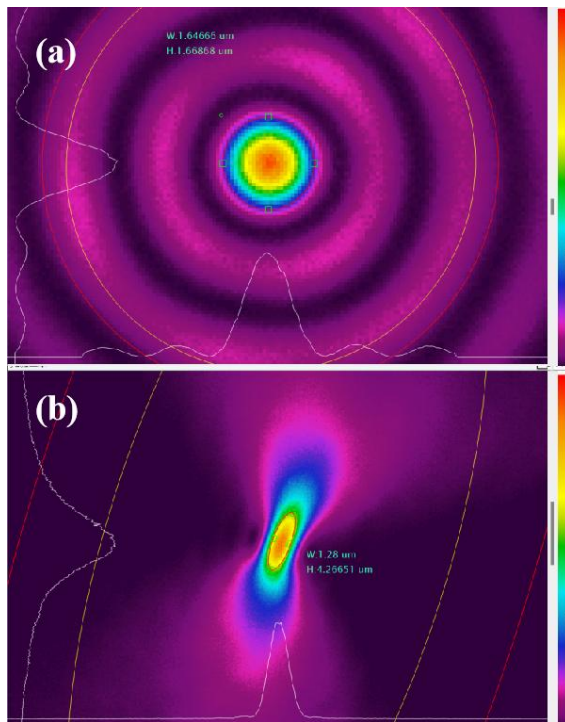


Fig. 2 Intensity distribution of the (a) symmetric and (b) asymmetric Bessel beam.

Table 2 Measurement results of symmetric and asymmetric Bessel beam.

	Symmetric Bessel beam	Asymmetric Bessel beam
Length (μm)	1.65	4.27
Width (μm)	1.67	1.28

2.2 Methods

In this paper, a low-iron glass plate with a thickness of 1 mm is used for cutting. The sample was placed on a marble platform. The X-axis can move at a maximum speed of 1000 mm/s. Since the edge breakage of glass samples cut by the Bessel beam is relatively small, the cross-section roughness R_a is the best parameter to characterize the processing quality of glass samples. Symmetric and asymmetric Bessel beams were applied for glass cutting. The effects of the cutting speed, the incident laser power, and the defocusing distance on the average roughness of the cut cross-section were analyzed. A color 3D laser scanning confocal microscope (KEYENCE, VK-X3050, Japan) with a resolution of 1 nm was employed to observe the cut section of glass and the top ablation holes. The repetition accuracy of height and width at 50X is 20 and 50 nm respectively. The results were all measured at 50X magnification. It also can measure the surface morphology and roughness of the cross-sections. In addition, the partial morphology of the glass cross-section and holes under different power and processing point spacing were characterized using a FIELD scanning electron microscope (HITACHI, S-4800, Japan).

3. Results and discussion

In the experiment, low-iron ultra-white glass with a thickness of 1 mm was obtained from China Southern Glass. The visible light transmittance is above 91%, and the iron content is stably controlled below 150 ppm. The glass was cut using symmetric and asymmetric Bessel beams, respectively. The effects of the cutting speed and the incident laser power on the average roughness of the cut cross-section were analyzed.

3.1 Influence of defocusing distance on cutting quality

Defocusing distance is defined as the distance between the middle of the glass sample and the middle of the Bessel beam focal depth. When the central section is located below the middle of the glass, the value is positive. For the laser power of 22 W, repetition rate of 50 kHz, and cutting speed of 400 mm/s, the cross-section roughness of glass cutting samples with symmetric Bessel beam under different defocusing positions in the range of 300 ~ 1300 μm was obtained. It can be seen that the roughness is around 0.4 and 0.5 μm from Table 3. The experimental results indicate that there is no obvious correspondence between the cross-section roughness and defocusing distance. That is because the symmetric Bessel beam has a focal depth of about 8 mm while the asymmetric beam is 5 mm, which is much greater than the thickness of the glass.

Table 3 Influence of defocusing distance on the roughness of low-iron glass cutting samples.

Defocusing distance (μm)	300	500	700	900	1100
Roughness (μm)	0.51	0.53	0.51	0.44	0.54

3.2 Influence of cutting speed on cutting quality

Cross-sectional roughness variations with the cutting speed under symmetric and asymmetric Bessel beams were investigated. The characterization was performed as follows. Select four outlines on the glass section, as shown by the red line of R_{a1-4} in Figure 3(a). Taking R_{a1} as an example, 10 lines were taken around R_{a1} , and the line roughness was measured by confocal microscopy and then averaged as the line roughness of R_{a1} . In addition, the surface roughness of the section was measured in Figure 3(b). The linear roughness at different positions represents the influence of light intensity change on the topography of each region of the cross-section. The surface roughness characterizes the overall quality of the cross-section.

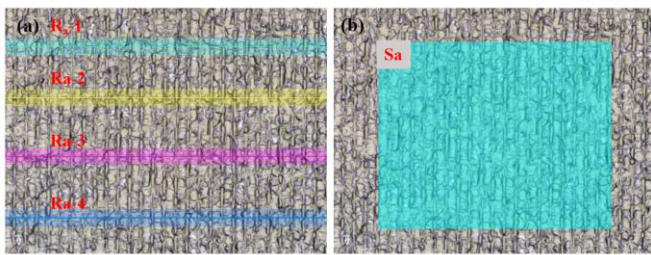


Fig. 3 Schematic diagram of sampling method for profile roughness of low-iron glass (a) cross-sectional morphology and profile selection for line roughness measurement and (b) surface roughness of the section.

The cutting results of different cutting speeds were obtained with a 50 kHz pulse-repetition frequency. The incident power is 45% and 70% of maximum laser power, respectively for asymmetric and symmetric Bessel beam conditions. When the laser repetition rate is constant, the hole spacing is proportional to the cutting speed and it increases with the speed. The optical microscope images of the upper surface of a glass sample with different cutting speeds from 400 mm/s~1000 mm/s based on asymmetric Bessel beam are shown in Figure 4. When the processing speed was 400 mm/s, micropores were connected to form an ablation groove. When the speed was more than 500 mm/s, the micropores were separated. When the processing speed was increased to 1000 mm/s, the micropores were more widely spaced, and cracks formed around the micropores.

From Figure 5(a), it can be seen that the roughness of the glass sample decreases first and then increases with the cutting speed for the symmetric Bessel beam. The smallest surface roughness of 0.6 μm was obtained when the cutting speed was 400 mm/s. When the cutting speed is less than 400 mm/s, the crack propagation is uncontrollable due to insufficient prestress. This is caused by the impact of dust and heat from the previous hole on the next hole during processing. When the cutting speed is less than 400 mm/s, the crack may not be formed or the crack is not parallel to the cutting direction, resulting in reduced effect. Therefore, using symmetric beams, the modifications have to be spaced closely in the dicing direction to properly cleave a sample. Typically, the spacing is of the same order as the central core diameter, and the cutting speed is limited by the laser pulse repetition rate.

For asymmetric Bessel beam, such beam generates intra-volume modifications with transverse crack

propagation in the dominant direction. Orientation of these modifications parallel to the dicing direction gives significant advantages in terms of processing speed and the maximum distance of a stable crack that can form is larger. It can be seen from Figure 5(b), when the cutting speed increases, the roughness does not increase significantly. Usually, when the cutting speed is high, the surface roughness is rather high. This is because the holes created by the symmetric Bessel beam are too far apart from each other, and large thermal stresses must be applied to separate the glass, leading to a lowered surface quality [21]. However, asymmetric beams make it easier to form cracks, and the force required for separation does not increase significantly after the speed increases. Thus, the roughness does not increase significantly. A minimum surface roughness of 0.6 μm was obtained at a cutting speed of 900 mm/s.

Our investigations show that the asymmetric Bessel beam can significantly improve the cutting speed, and plays an important role in the process of high-speed cutting glass. The high-resolution scanning electron microscopy (SEM) imaging of the top surface damage produced by the symmetric Bessel beam with a cutting speed of 400 mm/s, and asymmetric Bessel beam with a cutting speed of 900 mm/s is shown in Figure 6. The SEM reveals that the cleaved surface precisely follows the line through the laser-drilled nanochannels, which is the main reason for decreasing the brittleness of the material after processing and the decrease in sample roughness.

3.3 Influence of laser power on cutting quality

Due to the long depth of focus of the Bessel beam, the beam covered the entire cross-section of the samples. However, its light intensity distribution in the laser propagation direction is not completely uniform. The incident laser power affects the intensity distribution of the Bessel beam. In this section, the effect of different laser incident powers on the cutting quality was investigated based on symmetric Bessel beam and asymmetric Bessel beam. The roughness measurement results and cross sections for glass under symmetric and asymmetric Bessel beams with cutting speeds of 400 mm/s and 700 mm/s, respectively, are shown in Figure 7. For a symmetric Bessel beam, the relationship between roughness and laser power is similar to that of cutting speed. The minimum surface roughness of 0.5 μm is obtained when the laser power is 45% of maximum power. When the power continues to increase, over-high laser power may cause the material to adhere and melt in the laser processing area, which improves the separation strength of the material and the roughness of the section. For an asymmetric Bessel beam, the larger hole spacing avoids the influence of the former hole on the next hole at high power. In addition, the larger hole spacing also reduces material melting and crystallization in the processing area. The optimum results were obtained with the maximum laser power of 50%, with a surface roughness of 0.6 μm . When the power increases to 100%, the roughness value is almost unchanged compared to the symmetric Bessel beam. Cross-section images of cutting samples under different laser powers in asymmetric Bessel beams with a maximum power of 40%, 60%, 80%, and 100% are shown in Figure 8

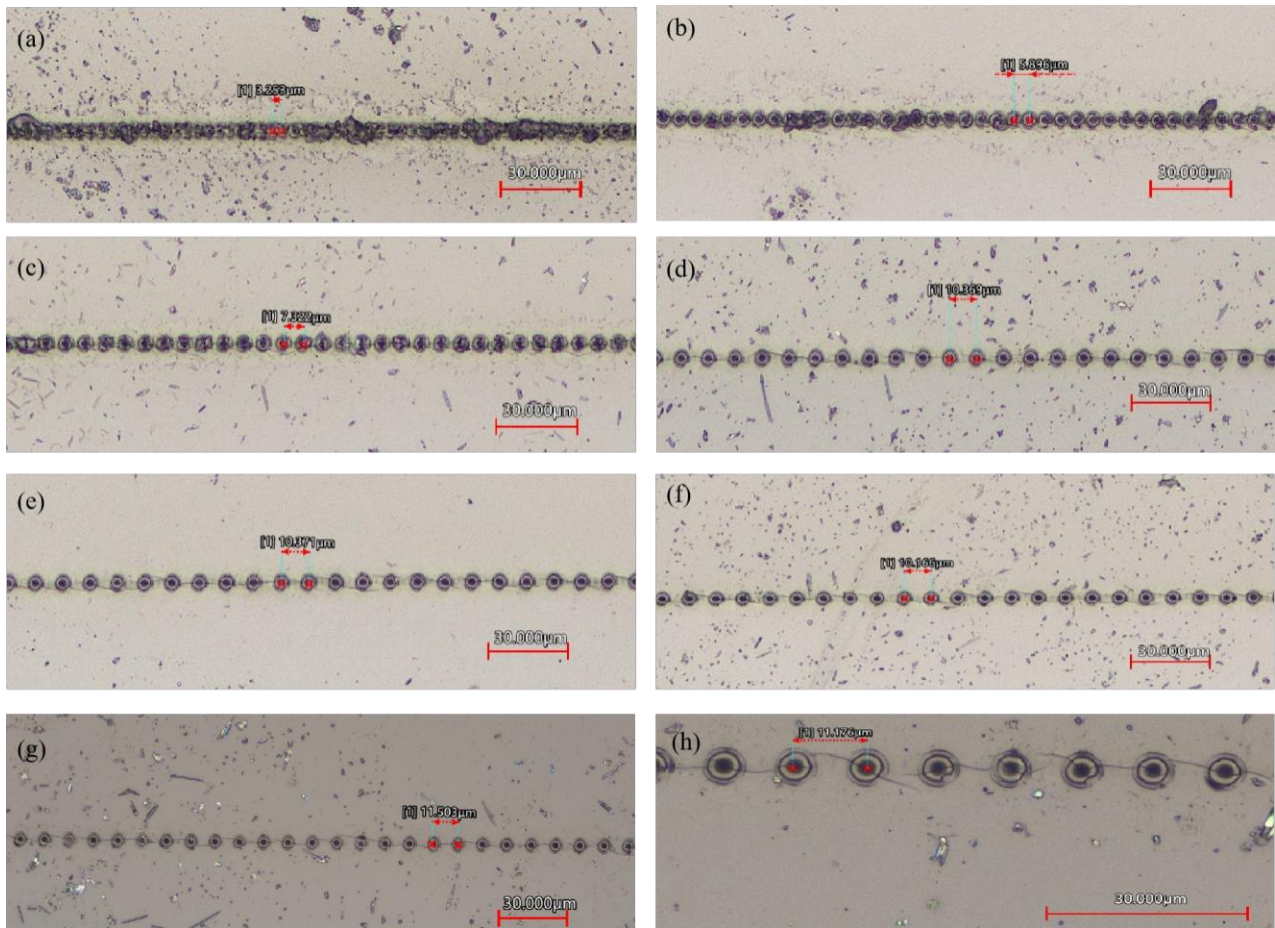


Fig. 4 Image of the upper surface of a glass sample with different cutting speed under asymmetric Bessel beam. (a) 400 mm/s, (b) 500 mm/s, (c) 600 mm/s, (d) 700 mm/s, (e) 800 mm/s, (f) 900 mm/s, (g) 1000 mm/s, (h) Partial magnification at 1000mm/s.

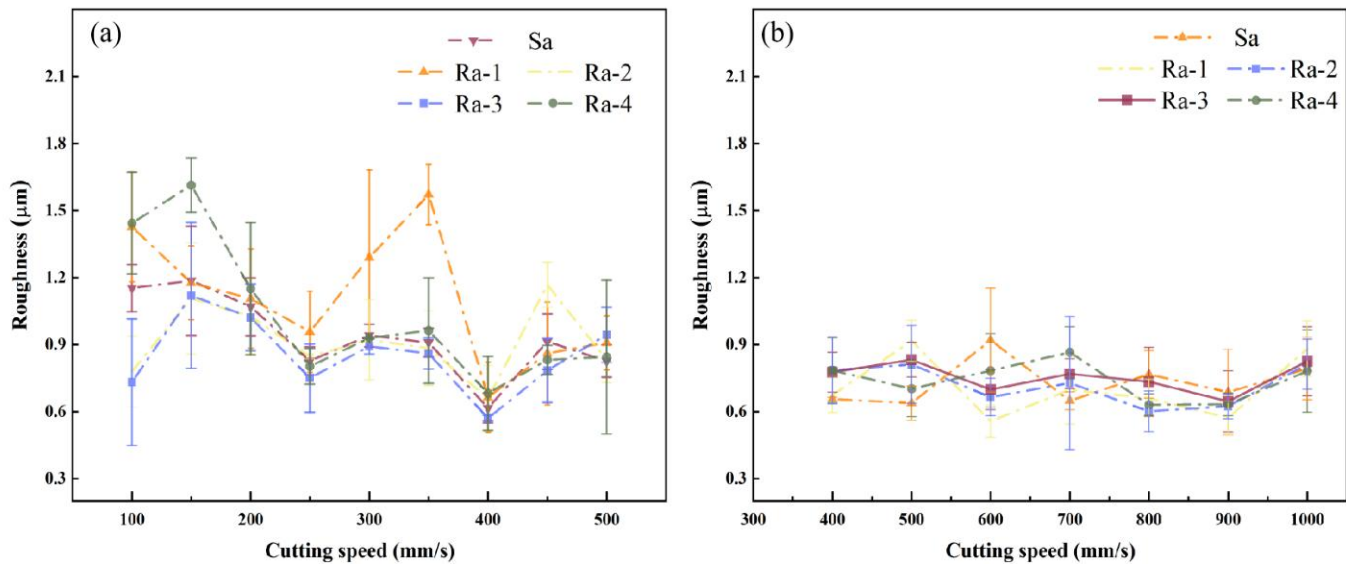


Fig. 5 Effect of cutting speed on the roughness of cutting samples cross-sections. (a) symmetric Bessel beam, (b) asymmetric Bessel beam.

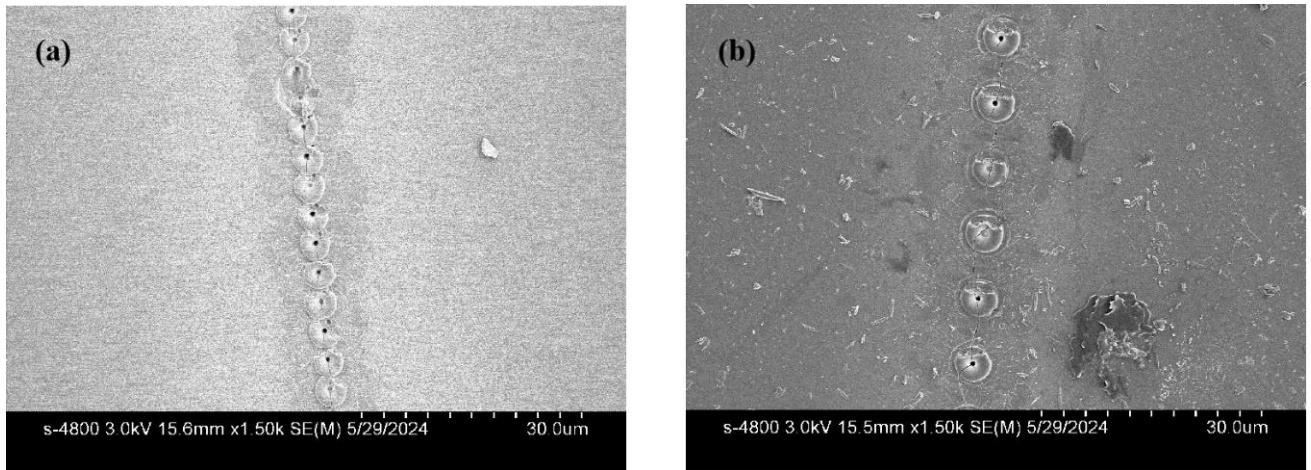


Fig. 6 SEM imaging of the top surface damage produced by (a) symmetric Bessel beam with cutting speed of 400 mm/s, and (b) asymmetric Bessel beam with cutting speed of 900 mm/s.

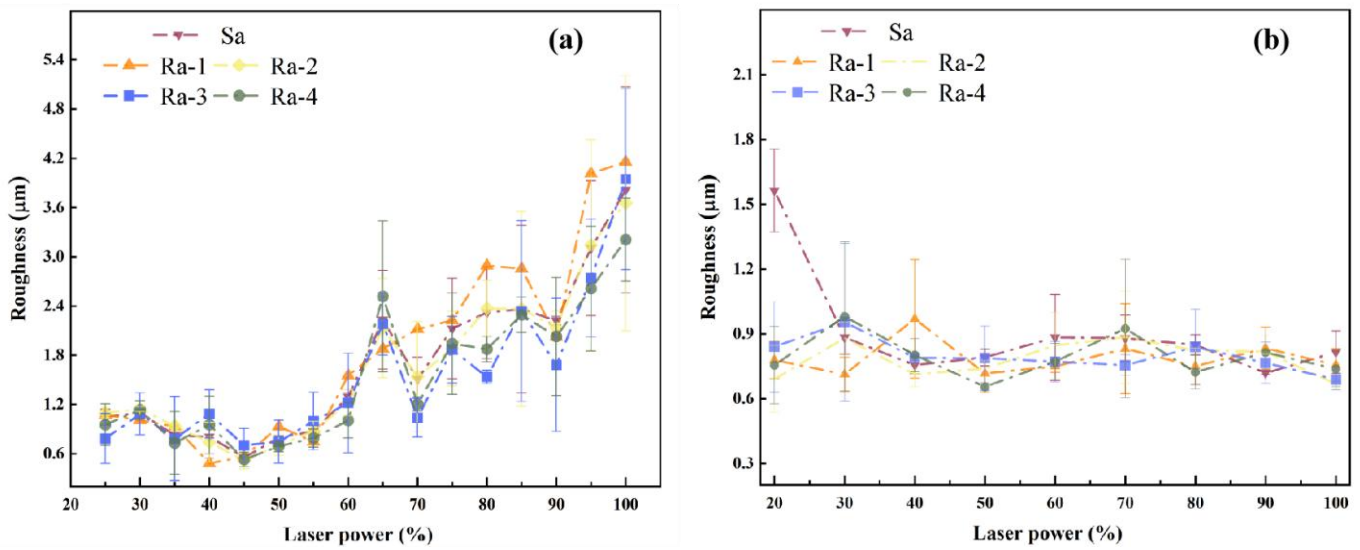


Fig. 7 Effect of laser power on the roughness of cutting samples cross-sections. (a) symmetric Bessel beam, (b) asymmetric Bessel beam.

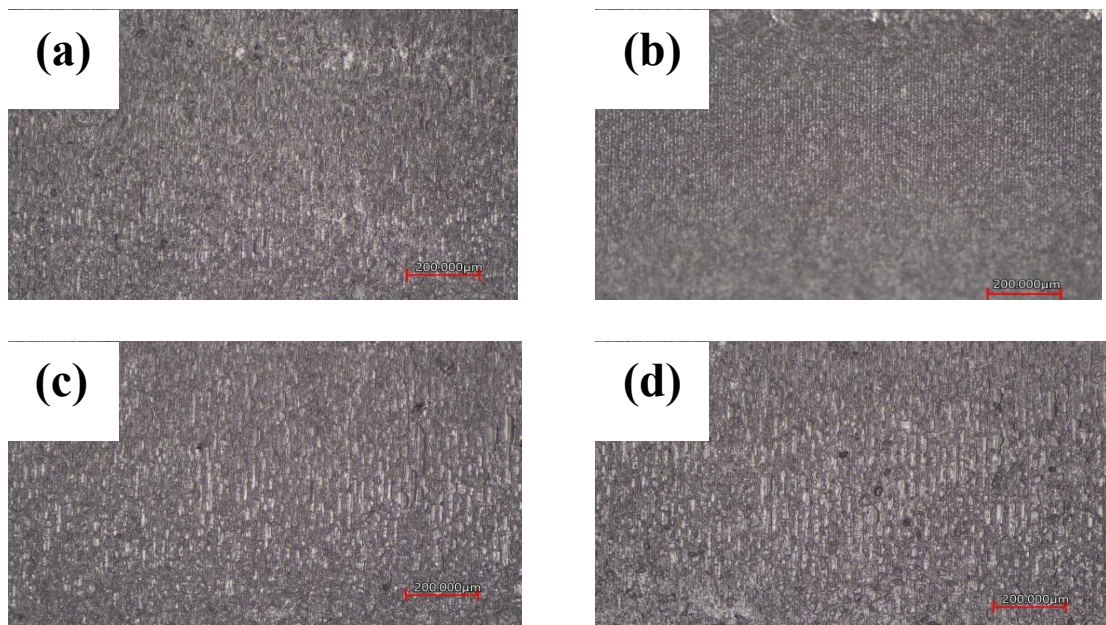


Fig. 8 Cross-sectional images of cutting samples under different laser power in asymmetric Bessel beam. (a) maximum power of 40%, (b) maximum power of 60%, (c) maximum power of 80%, (d) maximum power of 100%.

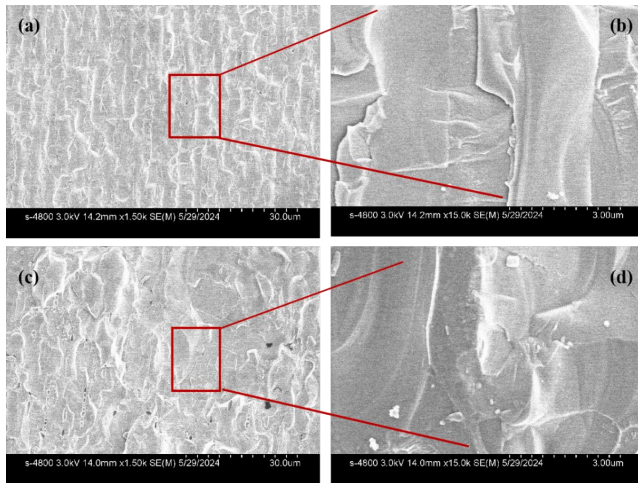


Fig. 9 SEM images of cutting samples under different laser power in asymmetric Bessel beam. (a) maximum power of 40%, (b) Partial magnification at maximum power of 40%, (c) maximum power of 80%, (d) Partial magnification at maximum power of 80%.

and some SEM images are presented in Figure 9, respectively. It can be clearly seen that when the incident energy was greater than 80%, the excessive laser incident energy led to the crystallization of the material in the machining region, which improved the roughness of the cross-section.

4. Conclusion

In this paper, the cutting experiments of low-iron ultra-white glass were carried out based on symmetric and asymmetric Bessel laser beams with different laser processing parameters. A series of characterization tests were performed on the cut samples and the results were analyzed. Firstly, the effect of processing speed (hole spacing) on the cross-section quality of the sample was analyzed. The results of cutting cross-section roughness and surface images show that the fracture of the glass sample is mainly caused by the propagation of cracks between holes. The crack propagation is difficult to form stably with the increase of hole spacing. For a symmetric beam, the minimum surface roughness of $0.6\ \mu\text{m}$ was obtained when the cutting speed was $400\ \text{mm/s}$. In addition, cracks are more likely to form between holes under an asymmetric beam, which reduces the influence of increasing hole spacing on roughness, and the higher cutting speed cutting of $900\ \text{mm/s}$ was achieved based on an asymmetrical beam with a minimum surface roughness of $0.6\ \mu\text{m}$. The experimental results show that the asymmetric Bessel beam can significantly improve the cutting speed, and plays an important application prospect in the processing of high-speed glass cutting.

Acknowledgments

This project was funded by the Natural Science Basic Research Program of Shaanxi (Program No. 2022JQ-399). Provision of the laser experimental setups by Anhui Boyi Laser Technology CO., LTD.

References

- [1] L. Zhou, A. Wanga, S. Wu, J. Sun, S. Park, and T.N. Jackson: Appl. Phys. Lett., 88, (2006) 83502.
- [2] S. Garner, S. Glaesemann, and X. Li: Appl. Phys. A. Mater., 116, (2014) 403.
- [3] L. Brusberg, S. Whalley, and C. Herbst: Opt. Express, 23, (2015) 32528.
- [4] H. Ohsaki and Y. kokubu: Thin Solid Films, 351, (1999) 1.
- [5] F. A. veer and Y. M. rodichev: Strength Mater+, 43, (2011) 302.
- [6] A. Ouchene, G. Mollon, M. Ollivier, X. Sedao, A. Pascale-Hamri, G. Dumazer, and E. Serris: Appl. Surf. Sci., 630 (2023).
- [7] Z. Q. Li, X. F. Wang, J. L. Wang, O. Allegre, W. Guo, W. Y. Gao, N. Jia, and L. Li: Opt. Laser Technol., 135, (2021) 106713.
- [8] K. Liao, W. J. Wang, X. S. Mei, and B. Liu: Ceram. Int., 48, (2022) 7.
- [9] J. Dudutis, L. Zubauskas, E. Daknys, E. Markauskas, R. Gvozdaite, G. Raciukaitis, and P. Gecys: Opt. Express, 30, (2022) 3.
- [10] M.A. Azmir and A.K. Ahsan: J. Mater. Process Technol., 198, (2008) 1.
- [11] G. Savriama, J. Mendez, L. Barreau, C. Boulmer-Leborgne, and N. Semmar: J. Laser Appl., 25, (2013) 52010.
- [12] S. Nisar, L. Li and M.A. Sheikh: J. Laser Appl., 25, (2013) 42010.
- [13] X. xie, C. Zhou, X. Wei, W. Hu, and Q. Ren: Optoelectron. Adv., 2, (2019) 180017.
- [14] J. Dudutis, J. Pipiras, R. Stonys, E. Daknys, A. Kilikevicius, A. Kasparaitis, G. Raciukaitis, and P. Gecys: Opt. Express, 28, (2020) 32133.
- [15] X. Sun, J. Zheng, C. Liang, Y. Hu, H. Zhong, and J.A. Duan: Appl. Phys. A, 125, (2019) 1.
- [16] K. Liao, W. Wang, X. Mei, and B. Liu: Opt. Laser Technol., 142, (2021) 107201.
- [17] F. Ahmed, M. S. Lee, H. Sekita, T. Sumiyoshi, and M. Kamata: Appl. Phys. A, 93, (2008) 189.
- [18] F. Ahmed, M. Shamim Ahsan, M. Seop Lee, and M.B. Jun: Appl. Phys. A, 114, (2014) 1161.
- [19] Patent WO 2012/006736 A2, 19 January 2012.
- [20] K. Mishchik, R. Beuton, O. Dematteo Caulier, S. Skupin, B. Chimier, G. Duchateau, B. Chassagne, R. Kling, C. Honninger, E. Mottay, and J. Lopez: Opt. Express, 25, (2017) 26.
- [21] R. M. Herman and T. A. Wiggins: Opt. Soc. Am., 8, (1991) 6.
- [22] M. K. Bhuyan, F. Courvoisier, P. A. Lacourt, M. Jacquot, R. Salut, L. Furfaro, and J. M. Dudley: Appl. Phys. Lett., 97, (2010) 081102.
- [23] H. Shin and D. Kim: Opt. Laser. Technol., 129, (2020) 106307.
- [24] P. Balage, T. Guilberteau, M.Lafargue, G. Bonamis, C. Hönninger, J. Lopez, and I. Manek-Hönninger: Micromachines, 14, (2023) 1650.
- [25] K. Mishchik, R. Beuton, O. Dematteo Caulier, S. Skupin, B. Chimier, G. Duchateau, B. Chassagne, R. Kling, C. Honninger, E. Mottay, and J. Lopez: Opt. Express, 25, (2017) 26.

- [26] R. Meyer, R. Giust, M. Jacquot, J. M. Dudley, and F. Courvoisier: Appl. Phys. Lett., 111, (2017) 231108.
- [27] J.H. McLeod: J. Opt. Soc. Am., 44, (1954) 592.
- [28] R. Meyer, M. Jacquot, R. Giust, J. Safioui, L. Rapp, L. Furfaro, P. A. Lacourt, J. M. Dudley, and F. Courvoisier: Opt. Lett., 42, (2017) 21.
- [29] R. Meyer, R. Giust, M. Jacquot, J. M. Dudley, and F. Courvoisier: Appl. Phys. Lett., 111, (2017) 231108.
- [30] Juozas Dudutis, Rokas Stonys, Gediminas Raciukaitis, and Paulius Gcecys: Opt. Express, 26, (2018) 3.
- [31] D. Juozas, S. Rokas, R. Gediminas, and G. Paulius: Opt. Las. Tech., 111, (2019) 331.
- [32] Y.T. Liu, L.Z. Hu, Q.Q. Guo, Y.Q. Hou, L. Lü, E. L. Gurevich, and A. Ostendorf: Proc. of SPIE, Vol. 12762, (2023) 1276205.

(Received: June 28, 2024, Accepted: January 19, 2025)